Electronic Supplementary Information

Simulation of osmotic energy conversion in nanoporous materials: a concise single-pore model

Feilong Xiao,[a] Danyan Ji,[b] Hao Li,[a] Jialiang Tang,[a] Yaping Feng,[b] Liping Ding,[c] Liuxuan Cao,*[a] Ning Li,[a] Lei Jiang[b] and Wei Guo*[b]

[a] College of Energy, Xiamen University, Xiamen, Fujian 361005, P. R. China.

[b] CAS Key Laboratory of Bio-inspired Materials and Interfacial Science, Technical Institute of Physics and Chemistry, Chinese Academy of Sciences, Beijing 100190, P. R. China.

[c] Center for Physiochemical Analysis and Measurement, Institute of Chemistry, Chinese Academy of Sciences, Beijing 100190, P. R. China.

* To whom correspondence should be addressed: wguo@iccas.ac.cn (Wei Guo), caoliuxuan@xmu.edu.cn (Liuxuan Cao).

Table of the content:

1. Numerical simulation.

1.1 Governing equations

In the work, the ion transport properties of nanopores are simulated under the framework of continuum model based on the coupled Poisson-Nernst-Plank (PNP) equations.[1] The continuum dynamics equations assume that the transport coefficients are independent of position and time, and the state variables such as temperature and density do not vary appreciably in the system.[2]

The ion transport properties of a charged nanopore can be described by Nernst-Planck equation as follow:[3]

$$\overrightarrow{j_i} = -D_i(\nabla c_i + \frac{z_i e c_i}{k_B T}\nabla\Phi), \qquad i=+,\ -. \tag{S1}$$

where i stands for the ion specie, $\overrightarrow{j_i}$ is the local ionic flux, D_i is the diffusion coefficient, c_i is the local ion concentration, z_i is the valence, Φ is the local electrical potential, k_B, T, e, represent respectively for the Boltzmann constant, the temperature, the electron charge as their usual meanings.

The relationship between the electric potential and ion concentration is governed by the Poisson equation:

$$\nabla^2\Phi = -\frac{1}{\varepsilon}\sum_i z_i e c_i, \qquad i= +,\ -. \tag{S2}$$

where ε is the dielectric constant of the electrolyte solution.

The steady-state solution satisfies the continuity equation:

$$\nabla\cdot\overrightarrow{j_i} = 0, \qquad i=+,\ -. \tag{S3}$$

By the treatment of the solution of equations, the calculated results, including electric potential, ion flux, and ion concentration distribution can be obtained.

1.2 Computational domain and boundary conditions

The boundary condition for potential Φ is given by the Gauss law:

$$-\overrightarrow{n}\cdot\nabla\Phi = \frac{\sigma_s}{\varepsilon} \tag{S4}$$

where $\vec{n}$ stands for the unit vector in normal direction. The local ion flux $\vec{j}_i$ has the zero normal components at boundaries, which means the flux is zero through the wall:

$$\vec{n}\cdot\vec{j}_i = 0, \qquad i = +, -. \tag{S5}$$

Then, the current density of the ion species is obtained by the following equation:

$$\vec{i}_i = z_i e \vec{j}_i, \qquad i = +, -. \tag{S6}$$

Finally, the total current through the nanopores can be calculated by integrating the ionic current density over the cross section of the nanopores:

$$\vec{I}_i = \int \vec{i}_i dS, \qquad i = +, -. \tag{S7}$$

1.3 Thermodynamic analysis

The Gibbs free energy loss induced by solution mixing can be expressed as follow:

$$dG = -\frac{RT}{F}\ln\frac{a_H}{a_L}\,(|I_+| + |I_-|)\,dt \tag{S8}$$

where dt is an infinitesimal time unit, $\alpha_{H/L}$ is the chemical activity of the ion species in the reservoir, I_+ and I_- is the ion flux contributed by cations and anions respectively. Through membranes based osmotic energy conversion, the Gibbs free energy can partly be converted into electric work (dW):

$$dW = I_{net}\,\varepsilon_j\,dt \tag{S9}$$

where I_{net} is the net current generated by cations and anions, defined as $I_{net} = |I_+| - |I_-|$, ε_j is the membrane potential:

$$\varepsilon_j = (t_+ - t_-)\frac{RT}{F}\ln\frac{\alpha_H}{\alpha_L} \tag{S10}$$

The ion transfer number for cations (t_+) is:

$$t_+ = \frac{|I_+|}{|I_+| + |I_-|} \tag{S11}$$

Combining equation S9 and S10, dW can be expressed as:

$$dW = \frac{RT}{F}\ln\frac{a_H}{a_L}\frac{(|I_+|-|I_-|)^2}{|I_+|+|I_-|}dt \tag{S12}$$

So the maximum output power (P_{max}) can be expressed as:

$$P_{\max} = \frac{1}{4}\frac{dW}{dt} = \frac{(|I_+|-|I_-|)^2}{|I_+|+|I_-|}\frac{RT}{4F}\ln\frac{\alpha_H}{\alpha_L} \tag{S13}$$

2. Model parameters.

The 2D planar models are used to simulate osmotic energy conversion in nanoporous systems. Model 1# (Fig. S1) and model 2# (Fig. S2) are the single-pore model and multi-pore model, respectively. The reservoir size b is fixed to 2 μm, and a_0, a_1, a have a series of values listed in Table S1. When a_0 and a are larger than 1000 nm, which is considered large enough in the literature that it will not affect the calculated results,[4] the models are called with infinite reservoir. Otherwise, when they are set small enough, for example, in Fig. 1-Fig. 4, a is set to 300 nm, which equals the distance of adjacent nanopores with the pore density of 3×10^8 pores/cm^2, the model is called with finite reservoir. The pore length L=1 μm, the pore diameter D=10 nm, and the surface charged density σ=-0.06 C/m^2, which is consistent with existing literature.[5, 6] The detailed parameters setting are shown in Table S1. Due to the negatively charged in nanopore wall, the nanopore is cation selectivity. The concentration difference applied in all models are 300 | 1 mM.

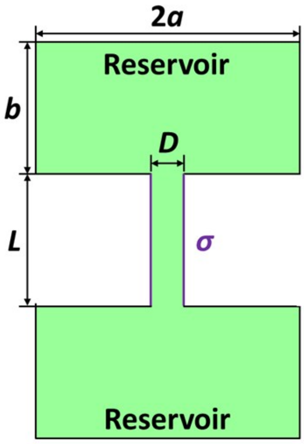

Fig. S1 Schematic illustration of the 2D planar single-pore model (model 1#). Two reservoirs are connected by single nanopore.

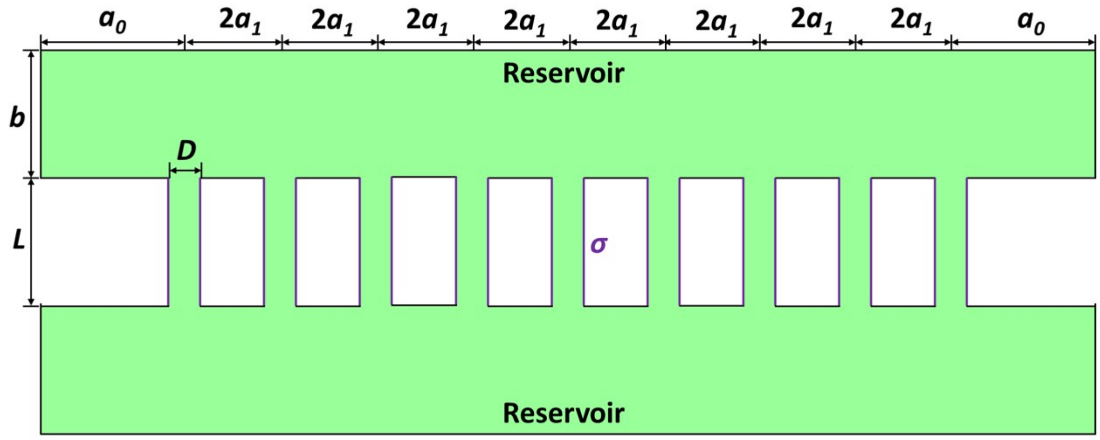

Fig. S2 Schematic illustration of the 2D planar multi-pore model (model 2#). Two reservoirs are connected by a series of nanopores. The pore number can be set from three to nine.

Table S1 List of model parameters.

a (μm)	a_0 (μm)	a_1 (μm)	b (μm)	L (μm)	D (nm)	σ (C/m^2)	Parameters involved in the manuscript
0.3 for finite reservoir; 4 for infinite reservoir	4	0.3	2	1	10	-0.06	Fig. 1-2 and Fig. S3-S4
0.3	4	0.3	2	1	10	-0.06	Fig. 3-4
0.03-5	4	0.3	2	1	10	-0.06	Fig. 5
0.3	0.3	0.3	2	1	10	-0.06	Fig. S6
/	0.3	0.3	2	1	10	-0.06	Fig. S7
/	4	0.3	2	1	10	-0.06	Fig. S8
/	0.3	0.3	2	1	10	-0.06	

3. Effective concentration difference (ECD).

We calculated the ECD of the central pore in the multi-pore models with infinite reservoir. With the increasing of pore number, the pore-pore interactions become more serious, and induce stronger ion concentration polarization (ICP) at the central pore end, which presents as ion concentration reduction at the high-concentration end (Fig. S3a) and ion concentration enhance at the low-concentration end (Fig. S3b), leading to the degradation of the ECD (Fig. S3c). The curve gradually drops down as the pore number increasing, and finally approach the value of single-pore model with finite reservoir condition. The applied concentration difference is 300 | 1 mM.

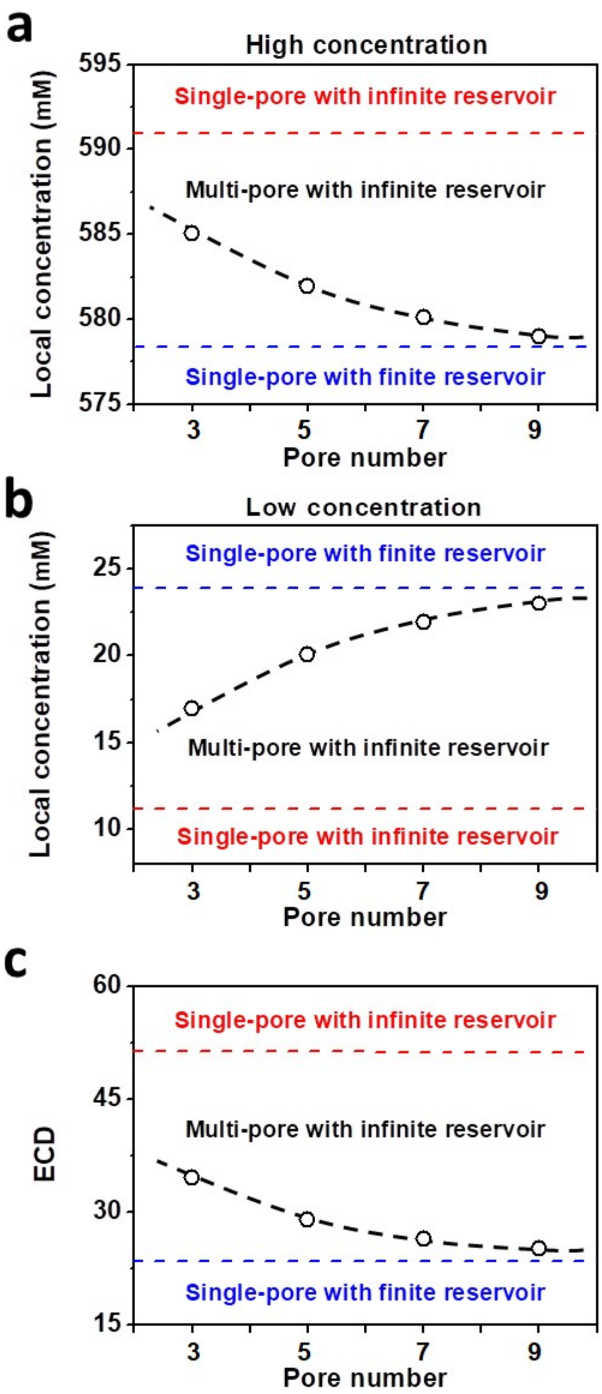

Fig. S3 The ion concentration polarization and effective ion concentration difference. (a, b) With the increment of pore number, the pore-pore interactions induce severe ICP, which result in ion concentration enhance at the low-concentration end and ion concentration reduction at the high-concentration end; (c) The degradation of the ECD of the central pore. The curve gradually drops down as the pore number increasing, and finally approach the value of single-pore model with finite reservoir condition. The applied concentration difference is 300 | 1 mM.

4. ECD and ion selectivity of nine-pore model with infinite reservoir.

We calculated the ion transport properties of individual pores in the nine-pore model with infinite reservoir condition. The central pore which is mainly influenced by the pore-pore interaction gets the lowest diffusion current (Fig. S4a). As additional remarks, the diffusion currents of inner pores approach that of single-pore model with finite reservoir. It means the single-pore model with finite reservoir is similar to the inner pores in multi-pore models. The pore-pore interaction also causes significant ICP at the nanopores end, and eventually leads to the degradation of the ECD and the ion selectivity through the nanopores (Fig. S4b and Fig. S4c). The ECD and ion selectivity of the central pore have a large difference from the single-pore with infinite reservoir, and get close to the value of the single-pore model with finite reservoir.

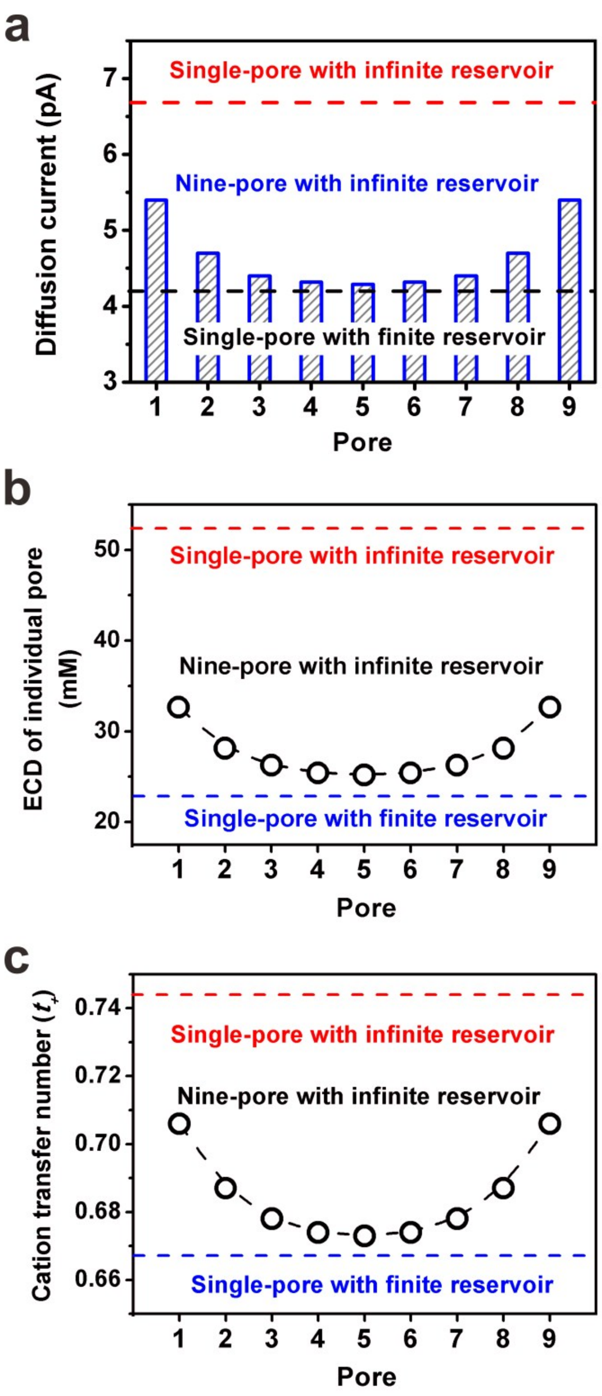

Fig. S4 The diffusion current, effective ion concentration difference (ECD) and cation transfer number of individual nanopores. (a) The diffusion currents of inner pores approach that of single-pore model with finite reservoir. (b) The central pore which mainly influenced by the pore-pore interaction gets the lowest ECD and the pores close to the boundary obtain the relatively high ECD. ECD of inner pores finally approach the single-pore model with finite reservoir. (c) The trend of cation transfer number is similar.

5. Diffusion current generated by multi-pore models with finite reservoir.

In the multi-pore models with finite reservoir, the diffusion current generated by individual pores are the same, and equal to the single-pore with finite reservoir. When the reservoir width of single-pore model equals to the distance between the adjacent pores in porous models, the single-pore model is equivalent to a pore unit in the multi-pore models. Setting proper reservoir is important to simulate the porous nanofluidic systems. When the solution reservoirs are regulated with different geometric sizes, the different pore-pore interaction (pore density) in porous nanofluidic systems can be simulated.

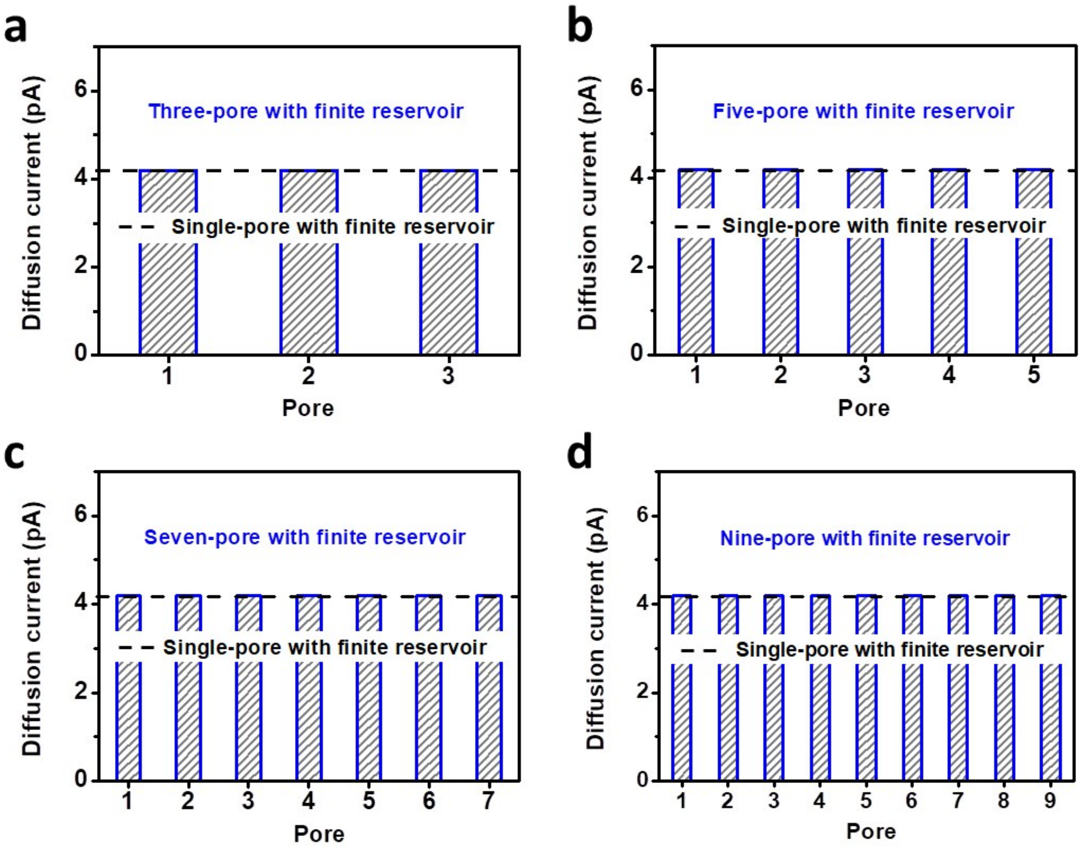

Fig. S5 The diffusion current through individual nanopores. (a-d) By setting the multi-pore models with finite reservoir, the diffusion current generated by individual pores are the same, and are identical to that of single-pore model with finite reservoir. In this case, the single-pore model is equivalent to a pore unit in the multi-pore model.

6. Local ion concentration distribution in the models with finite reservoir.

We calculated the local ion concentration distribution in the high-concentration reservoir of the multi-pore models with finite reservoir. The ion concentrations appear periodic change. The local ion concentration distributions at the pore entrance in different porous systems are the same. The local ion concentration distribution is not affected by the increasing pore number in the simulation models.

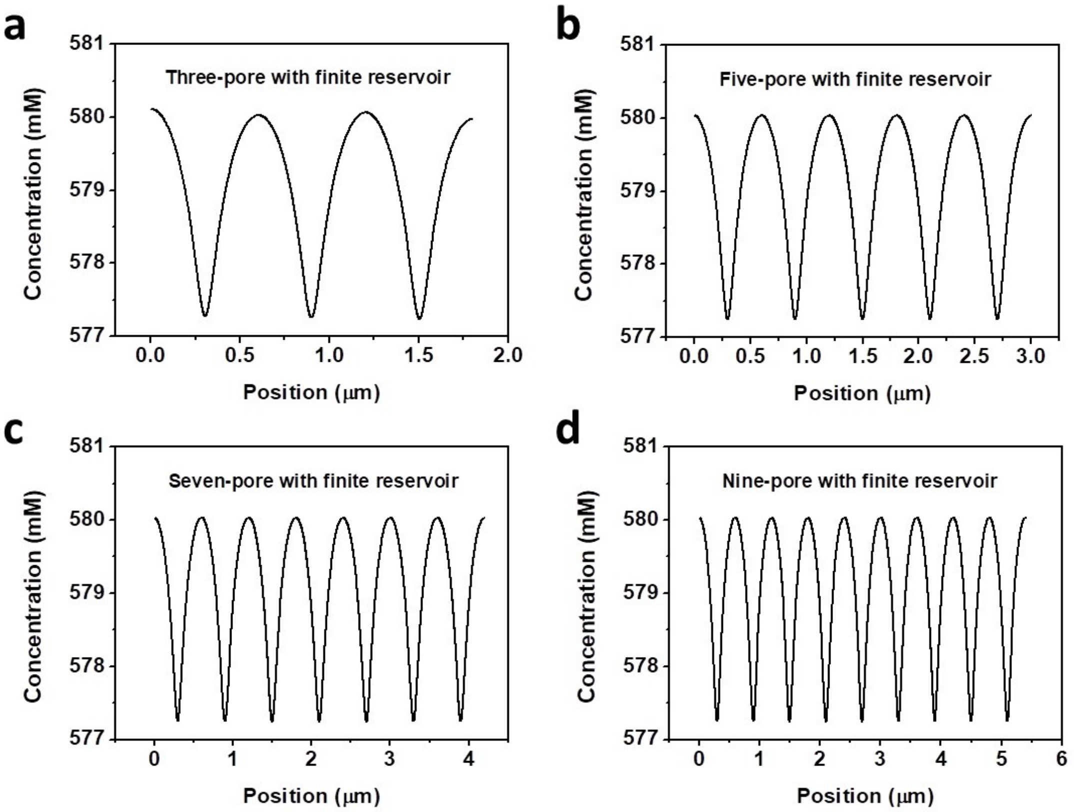

Fig. S6 The local ion concentration distribution in the multi-pore models with finite reservoir. (a-d) The local ion concentration distribution keeps periodic change in the multi-pore model with finite reservoir, which is not affected by the pore number in the simulation models.

7. Local ion concentration distribution in nine-pore model.

In the nine-pore model with infinite reservoir, the central pore is mainly affected by pore-pore interaction. When finite reservoir condition is applied, the local ion concentration distribution appears periodic change. The ion concentration distribution of the central pore in nine-pore model with infinite reservoir is close to that of nine-pore model with finite reservoir condition. For the central pore in the nine-pore model with infinite reservoir, the pore-pore interaction is simulated by inducing the n-th orders of nearest neighbouring nanopores to take the influence brought by the surrounding nanopores into consideration. For the individual pores in the nine-pore model with infinite reservoir, the pore-pore interaction is simulated by infinite reservoir boundary condition. The models (including single-pore and multi-pore) with finite reservoir condition can accurately simulate the inner pores of multi-pore nanofluidic systems.

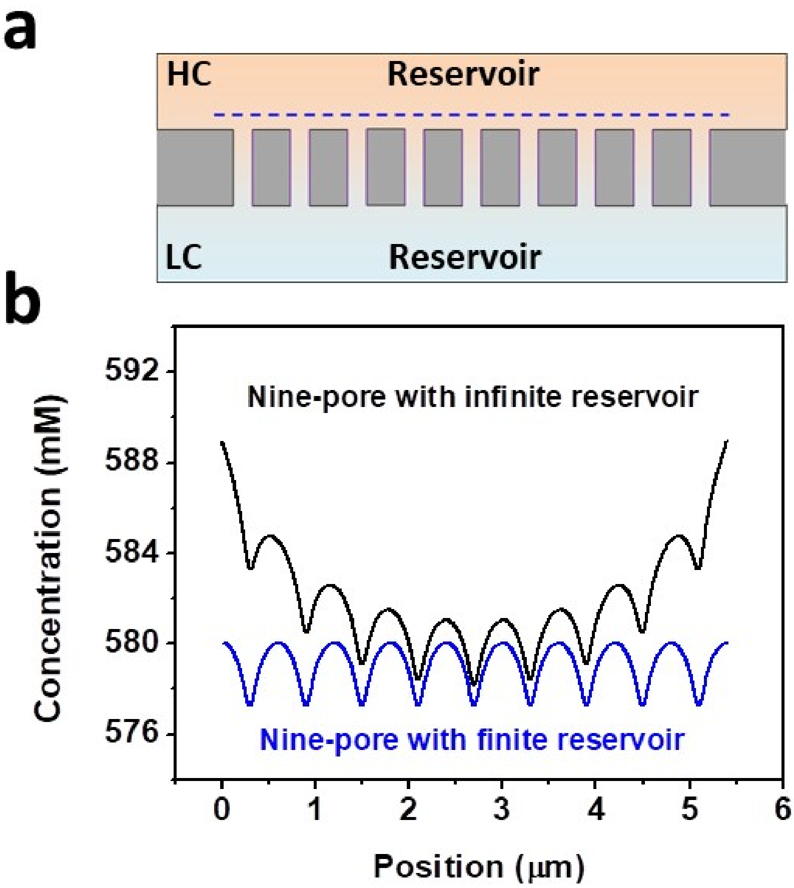

Fig. S7 The local ion concentration distribution in the high concentration side of nine-pore model (blue dash line). (a) Schematic illustration of the simulation models. (b) In the nine-pore model with finite reservoir, the local ion concentration distribution keeps periodic change. Because the central pore of nine-pore model with infinite reservoir is mainly affected by pore-pore interaction, the ion concentration distribution gets close to that of the nine-pore model with finite reservoir.

8. Appropriate reservoir size under other pore densities.

We calculated the diffusion current generated by the nine-pore models under other pore densities ranging from 1×10^6 to 1×10^9 pores/cm^2 (Table S2). By comparing the diffusion current obtained with the single-pore model and with the multi-pore model, the appropriate reservoir size for the single-pore model is determined. The results show that the appropriate reservoir size roughly equals to the inter-pore distance under all tested pore densities.

Table S2 Appropriate reservoir size of single-pore model and inter-pore distance under other pore density. The concentration difference is 300|1 mM.

Pore density (pores/cm^2)	Single-pore model (nm)	Multi-pore model (nm)
1×10^6	10002	10000
1×10^7	3220	3200
3×10^8	625	600
1×10^9	335	320

9. References

1. N. Modi, M. Winterhalter and U. Kleinekathofer, *Nanoscale*, 2012, **4**, 6166.
2. B. D. Kang, H. J. Kim, M. G. Lee and D. K. Kim, *Energy*, 2015, **86**, 525.
3. A. N. Chatterjee, D. M. Cannon, E. N. Gatimu, J. V. Sweedler, N. R. Aluru and P. W. Bohn, *J. Nanopart. Res.*, 2005, **7**, 507.
4. C.-Y. Lin, F. Chen, L.-H. Yeh and J.-P. Hsu, *Phys. Chem. Chem. Phys.*, 2016, **18**, 30160.
5. J. Cervera, B. Schiedt, R. Neumann, S. Mafé and P. Ramírez, *J. Chem. Phys.*, 2006, **124**, 4653.
6. I. Vlassiouk, S. Smirnov and Z. Siwy, *Nano Lett.*, 2008, **8**, 1978.